SUPPLEMENTARY MATERIAL

Interleukin-9 Mediates Chronic Kidney Disease-dependent Vein Graft Disease: a Role for Mast Cells

Lisheng Zhang,[1] Jiao-Hui Wu,[1] James C. Otto,[2] Susan B. Gurley,[3] Elizabeth R. Hauser,[4] Sudha K. Shenoy,[1,5] Karim Nagi,[1,5] Leigh Brian,[1] Virginia Wertman,[1] Natalie Mattocks,[3] Jeffrey H. Lawson,[2] Neil J. Freedman[1,5]

Departments of Medicine ([1]Cardiology, [3]Nephrology), [2]Surgery, [4]Biostatistics and Bioinformatics, [5]Cell Biology and the [4]Molecular Physiology Institute
Duke University Medical Center, Durham, North Carolina, USA
[4]Cooperative Studies Program Epidemiology Center
Durham Veterans Affairs Medical Center, Durham, North Carolina, USA

SUPPLEMENTARY MATERIALS AND METHODS

Mice

All mice were C57BL/6J, housed in a barrier facility on a 12-hour light-dark cycle; they received ad libitum water and standard chow LabDiet 5053 (irradiated). All animal experiments were performed according to protocols approved by the Duke Institutional Animal Care and Use Committee; these protocols complied with the *Guide for the Care and Use of Laboratory Animals* (National Academies Press, 2011).

Nephrectomy model of CKD

The 5/6^{ths} nephrectomy procedure was performed in two sequential operations, modified from published protocols.[1-3] For analgesia, mice were treated with acetaminophen (300 mg/kg daily for 48hrs pre-op and post-op via drinking water), and injected with buprenorhphine SR (0.5 mg/kg at the time of surgery). Anesthesia with pentobarbital (50 mg/kg i.p.) was used for all surgeries. The left partial nephrectomy was performed first: we incised left flank through the dorsoventral muscles, and then performed lateral left renal capsulotomy (the capsule subsequently contracts toward the hilum). Next, the upper and lower poles of the left kidney were removed, leaving behind the segment around the hilum. Hemostasis on the cut renal surface was achieved by cauterization and/or Gelfoam®. The musculofascial and skin incisions were closed with 5-0 vicryl suture. Ten days later, we used a similar approach for right total nephrectomy: the renal pedicle was ligated with 5-0 vicryl, the vessels and ureter were severed, and the entire kidney was removed. For mice undergoing sham surgery, we performed only bilateral renal capsulotomy. For mice undergoing 1/3rd nephrectomy, we performed the left partial nephrectomy described above and a right renal capsulotomy. After the second stage of the nephrectomy surgeries, mice were allowed to recover for 2 wk before undergoing either GFR measurement or carotid interposition vein grafting. All mice in 5/6ths nephrectomy and corresponding control cohorts (sham nephrectomy or 1/3rd nephrectomy) were matched for age and sex; they did not differ with regard to weight pre- or post-operatively (22-23 gm prior to vein graft surgery). Blood pressure in C57BL/6J mice is not altered by 5/6ths nephrectomy.[4,5] All control-GFR mice for vein graft surgeries were subjected to 1/3rd nephrectomy, which does not alter GFR (because total unilateral nephrectomy does not alter GFR).[2]

GFR measurement

Under 2% isoflurane anesthesia, CKD and control mice matched for age and gender were injected retro-orbitally with sterile FITC-inulin at time 0; saphenous vein blood (~10 µl) was collected into heparinized capillary tubes 3, 7, 10, 15, 35, 55, and 75 min afterwards. Plasma fluorescence was determined and GFR calculations were performed as described.[6]

Carotid interposition vein grafting

Interposition vein graft surgery was performed as we described previously,[7-11] on mice that previously underwent 5/6ths or 1/3rd nephrectomy. All mice were wild-type (WT), C57BL/6J mice. Inferior venae cavae from donor mice were harvested after pentobarbital-induced anesthesia (50 mg/kg, i.p.). The inferior vena cava was stored in heparinized PBS while the recipient of the vein graft was anesthetized (pentobarbital, 50 mg/kg, i.p.), shaved and prepared for surgery. The donor inferior vena cava was anastomosed end-to-side to the right common carotid artery of control-GFR or CKD recipient mice. After both vein graft anastomoses were secured, the intervening common carotid artery was ligated and cut, thereby stretching the IVC graft. All vein graft donors and recipients were matched for gender and age (10-15 wk old). Grafts were harvested 4 weeks postoperatively from pentobarbital-anesthetized mice (50 mg/kg, i.p.), after perfusion-fixation with 3.7% formaldehyde (20 min, 80 mm Hg pressure), and prepared for histochemical and immunofluorescence analysis as we described previously.[7-9]

Histology

Paraffin-embedded vein grafts were sectioned at 5 μm, from the distal or middle third of the vein graft specimens; all vein graft groups were matched for section location. For morphometry, sections were stained with a modified Masson's trichrome and Verhoeff's elastic tissue stain that facilitates the simultaneous identification of collagen (green), elastin (black), cytoplasm (red), and nuclei (black).[7] Morphometry was performed on vein grafts by observers blinded to specimen identity, as we have described.[7,9,12] The neointimal/medial boundary was defined as the transition from the cytoplasm-rich, disorganized neointima to the collagen-rich media. The medial/adventitial boundary was defined as the transition from the more densely organized medial collagen to the less densely organized, vasa vasora-containing collagenous network of the adventitia. Neointimal area was measured as the cross-sectional area subtended by the luminal perimeter and the neointimal/medial boundary. Medial area was measured as the cross-sectional area subtended by the neointimal/medial and medial/adventitial boundaries. For each vein graft, lumen area was normalized to the cross-sectional area encompassed by the boundary between the media and the adventitia; this ratio was plotted as "lumen / total vein graft area".

Vein graft immunofluorescence was performed as described,[9,12] using rabbit IgGs specific for the following proteins: vascular cell adhesion molecule-1 (VCAM-1, Santa Cruz Biotechnology, sc-8304); proliferating cell nuclear antigen (PCNA, Santa Cruz Biotechnology, sc-7907); NFκB p65 (Santa Cruz Biotechnology, sc-109); NFκB p65 phosphorylated on the IκB kinase target Ser536 (Cell Signaling, monoclonal IgG #3033S); interleukin-9 (IL-9, Gene Tex, #GTX51537); IL-9 receptor-α (IL-9Rα, Santa Cruz Biotechnology, sc-1030); von Willebrand factor (vWF, DAKO, A0082); tryptase (mouse mast cell proteases [mMCPs] 6 and 7, Santa Cruz Biotechnology, sc-32889); mouse mast cell protease-5 (mMCP5, or "chymase", MyBioSource, Inc., MBS2002348). Goat IgG was used to detect TNF and CD3 (Santa Cruz Biotechnology, sc-1351 and sc-1127, respectively). Mouse monoclonal IgGs were used to immunostain TNF receptor-1 (TNFR1, Santa Cruz Biotechnology, sc-8436) and collagen I (Sigma-Aldrich, c2456). Alexa Fluor® 488-conjugated rat IgG_{2a} anti-mouse CD68 (Biolegend, #137012) was used to stain macrophages; non-immune Alexa Fluor® 488-conjugated rat IgG_{2a} was used for negative control sections. Negative control serial sections were incubated with equivalent concentrations of non-immune, isotype control IgG in lieu of primary antibody. Cyanine 3-conjugated 1A4 IgG (Sigma, C6198) was used to detect smooth muscle α-actin, as described.[9] The DNA-binding dye Hoechst 33342 (10 μg/mL, Invitrogen) was added to secondary antibody incubations.

Single microscopic fields were imaged for multiple fluorophores using narrow band-pass filter cubes on a Leica DM6 B light/fluorescence microscope, as described.[9,10,12] We compared vein graft protein expression between groups: control-GFR vs. CKD, control IgG-injected vs. anti-IL-9 IgG-injected. To do so, we stained and imaged vein grafts specimens from each group simultaneously, batch-wise. Identical exposure times and incident light intensities were used to visualize each specimen; images of each vein graft were captured with a Q charge-coupled device camera (Q Imaging, Inc.) at 200×. At this magnification only ~50% of each vein graft fit into a single photograph; consequently, immunofluorescence quantitation for each vein graft required 2 photographs (the results from which were averaged for each specimen).

Immunofluorescence was analyzed using NIH ImageJ software by observers blinded to specimen identity, as we described.[9,10] The "total" immunofluorescence signal for a particular vein graft (vein graft wall, neointima, etc.) was measured on samples incubated with a primary IgG targeting a specific protein. The "nonspecific" immunofluorescence was measured on a serial section incubated with an isotype negative control IgG. "Specific" immunofluorescence for each specimen was calculated by subtracting "nonspecific" from "total" immunofluorescence. Specific immunofluorescence was then normalized to (Hoechst 33342-stained) DNA fluorescence intensity (Hoechst 33342-stained) obtained in cognate portions of the same vein graft section—thereby normalizing protein immunofluorescence to cellularity.[9,10] These protein/DNA ratios were averaged among all vein grafts within each group; the ratios were then normalized to those obtained for the control samples within each immunostaining/imaging cohort.

The extent of vein graft re-endothelialization was determined as the percentage of luminal perimeter surfaced by von Willebrand factor-positive cells, as judged from vein graft cross sections measured by observers blinded to specimen identity, as we described.[10]

Toluidine blue stain for mast cells was performed as described previously.[13,14] Briefly, de-paraffinized 5-μm vein graft sections were stained with 0.1% (w/v) toluidine blue in 154 mmol/L NaCl/7% (v/v) ethanol, pH 2.5 for 2 min (25 °C), washed with water and then dehydrated with 95-100% ethanol, followed by xylene. Mast cells were identified by their metachromatic (purple) granules, which are distinct from the orthochromatic (blue) staining of all other cells. Mast cells were dichotomized as (a) quiescent, with densely packed in the cytoplasm, or (b) activated, or degranulating, with disgorged and loosely packed granules.[13,14] These mast cells were quantitated by observers blinded to specimen identity; a minimum of 100 mast cells per specimen were counted.

Confocal microscopy was performed as we described,[15] with a Zeiss LSM 510 META confocal microscope, to identify nuclear localization of the NFκB p65 subunit in the vein graft neointima and media. Sections were stained with rabbit IgG targeting the NFκB p65 subunit or non-immune rabbit IgG, followed by Alexa® 568-conjugated anti-rabbit IgG (Thermo Scientific) along with DRAQ5™ (to stain nuclear DNA [Alexis Biochemicals]). Confocal images were acquired such that each channel was scanned successively using filter sets for multitrack sequential excitation (568, and 633 nm) and emission (585-615 nm, Alexa® 568; 650 nm, DRAQ5). To facilitate reliable co-localization studies, a 100× oil objective was used, and a pin-hole for each channel was matched for airy units to set optical slice thickness at 1 μm.[16] Final processing of images was performed with Adobe Photoshop CS2 software; the brightness and contrast were adjusted for entire images and to the same extent for p65 and control IgG images.

Serum cytokine assays

To determine how CKD affects plasma cytokine levels and to determine how CKD serum affects endothelial cell proliferation, we harvested serum 2 wk after the final nephrectomy surgery from mice subjected to 5/6ths nephrectomy, sham nephrectomy, or 1/3rd nephrectomy. To determine the effects of anti-IL-9 IgG or cromolyn therapies on plasma cytokine levels, we harvested serum from CKD mice 4 weeks after vein graft implantation (and 2-3 days after the final injection of either anti-IL-9 IgG or cromolyn). Mice were anesthetized with pentobarbital and exsanguinated by ventricular puncture. Blood was allowed to coagulate in pyrogen-free tubes for 30 minutes at room temperature, and then centrifuged at 1,000 ×g (4 °C, 10 min). Supernatant serum was transferred to new tubes and spun again (1,000 ×g at 4 °C, 10 min); supernatant serum was aliquotted and stored at minus 80 °C until it was analyzed. Serum amyloid A concentrations were measured by ELISA with a kit from Biosource International, Inc., as we described.[12]

Mouse sera were analyzed in triplicate using the Bio-Plex Pro™ Mouse Cytokine Assay on a BioPlex 1036 Array Reader (BioRad, Inc). Individual sera from CKD (n = 13) versus control-GFR (n = 9) mice were compared in a single run (a single plate) of the Bio-Plex Pro™ Mouse Cytokine Assay, according to the manufacturer's instructions. Similarly, individual sera from anti-IL-9 IgG-injected (n = 7) versus control IgG-injected (n = 7) mice and cromolyn-injected versus saline-injected mice were compared in single runs of the Bio-Plex Pro™ Mouse Cytokine Assay. The Bio-Plex Pro™ Mouse Cytokine Assay detects 23 cytokines (or 22, if IL-12 p70 and p40 subunits are counted as a single cytokine): interleukin-1α (IL-1α), IL-1β, IL-2, IL-3, IL-4, IL-5, IL-6, IL-9, IL-10, IL-12(p40), IL-12(p70), IL-13, IL-17, KC (CXCL1), G-CSF (granulocyte colony-stimulating factor), IFNγ (interferon-γ), MIP-1α (CCL3), MIP-1β (CCL4), RANTES (CCL5), and TNF (tumor necrosis factor).

Systemic neutralization of IL-9

At the time of vein graft surgery, CKD mice were injected with one of 2 Armenian Hamster IgG_2/κ molecules: (a) D9302C12, which neutralizes IL-9,[17] or (b) control IgG, which binds no known mouse protein (BioLegend): 50 μg intravenously plus 250 μg i.p. Subsequently, mice were injected with the same IgG three times per week (300 μg i.p.)[17] until vein graft harvest 4 wk after implantation. (Hamster IgG is not immunogenic in mice.[18]) Mice were sacrificed for vein graft harvest 48-72 hours after the final injection of IgG.

Serum creatinine assay
Mouse sera were assayed for creatinine concentration using an enzymatic assay with a colorimetric endpoint (Creatinine Assay Kit, Sigma-Aldrich # MAK080),[19,20] according to the manufacturer's specifications. All mouse sera were run in triplicate, in a single assay.

Systemic treatment with cromolyn
To prevent mast cell degranulation in CKD mice, we treated mice with the mast cell stabilizer cromolyn as reported by others.[13,21] Cromolyn sodium (10 mg/ml, Teva Pharmaceuticals) was diluted 1:1 prior to intraperitoneal injection with 2× PBS (made from 10× PBS [VWR] and USP sterile water, Mediatech, Inc.). One day prior to vein grafting, CKD mice were injected i.p. with either PBS or cromolyn (50 mg/kg). After vein grafting, mice were injected with cromolyn or PBS twice per week for 4 weeks, after which vein grafts were harvested as described above.

Endothelial and smooth muscle cell proliferation
Aortas were harvested from mice anesthetized with pentobarbital (50 mg/kg, i.p.). Endothelial cells (ECs) and smooth muscle cells (SMCs) were isolated by enzymatic digestion and passaged as we described.[22] The purity of EC preparations was assessed by the prevalence of von Willebrand factor (vWF) immunofluorescence, which was ≥90%; three independently derived mouse EC lines were used in experiments. The purity of SMC preparations was assessed by the prevalence of smooth muscle α-actin staining, which was ≥90%; three independently derived mouse EC lines were used in experiments.

For EC growth experiments, we used 96-well plates coated with collagen I. ECs for the growth experiments were plated at 2.5×10^3 cells/well in "medium A": Dulbecco's modified Eagle medium (DMEM) containing 20% FBS (which was previously heat-inactivated), 1× L-glutamine, 1× non-essential amino acids, 1× sodium pyruvate (Invitrogen), 25 mmol/L Hepes (pH 7.4), 100 µg/ml heparin, 100 µg/ml EC growth supplement (Sigma-Aldrich), and 1% penicillin/streptomycin (Invitrogen). In parallel, the same pool of ECs was plated in medium A on the "standard curve" plate at serial 2-fold dilutions ranging from 2.5×10^3 to 10×10^3 cells/well. After 16 h, ECs were washed twice with "medium B", defined as medium A that lacks FBS. Next, ECs on the growth assay plate (sextuplicate wells) were re-fed with medium B lacking (control) or containing 20% (vol/vol) serum from three cohorts of mice (6 mice/cohort): (1) 5/6ths nephrectomized, (2) 1/3rd-nephrectomized, or (3) sham-nephrectomized. Both control and mouse serum-containing medium B also contained the same Armenian Hamster IgG_2/κ molecules used in the in vivo IL-9 neutralization experiment: either D9302C12, which neutralizes IL-9,[17] or control IgG, at 2 µg/ml ([final]). Parallel ECs on the standard curve plate were washed with PBS, stained with crystal violet (see below), and stored dry until the conclusion of the growth assay. ECs were incubated in this medium for 4 days (37 °C in a CO_2 incubator). Subsequently, ECs were washed with PBS and then stained with 0.5% (w/v) crystal violet in 5% (v/v) ethanol for 60 min. After extensive washing, ECs were dried completely, and EC-adsorbed crystal violet was dissolved in 40% acetic acid. The absorbance of each well was then read at 562 nm in sextuplicate, and corrected for the absorbance obtained in wells in which no ECs had been plated. EC protein was quantitated with a standard curve generated from crystal violet readings obtained from the standard control plate. The relationship between OD_{562} and EC number was linear from 0 to 10×10^3 ECs/well (data not shown). To determine the effect of mouse serum on EC proliferation, we subtracted from each well the number of ECs present in control wells containing just medium B. EC growth data were equivalent with mouse serum from sham-nephrectomized and 1/3rd-nephrectomized mice (data not shown).

SMCs were cultivated in medium D: DMEM with 10% fetal bovine serum (FBS) and 1% penicillin/streptomycin (Gibco). Prior to proliferation assays, confluent SMCs incubated for 24 hr in serum-free medium (DMEM with 20 mmol/L Hepes pH 7.4, 0.1% (w/vol) fatty acid-free bovine serum albumin (Sigma-Aldrich), 1% penicillin/streptomycin); they were then trypsinized and plated in 96-well plates at 2×10^3 cells/well in medium D. Four hours later, SMCs were washed with PBS and re-fed with one of the following media: (a) DMEM with 2.5% FBS and 1% penicillin/streptomycin, lacking (control)

or containing IL-9 (R&D Systems) at 600 pg/mL; (b) DMEM with 10% (vol/vol) CKD mouse serum and 1% penicillin/streptomycin; (c) DMEM with 10% (vol/vol) control-GFR mouse serum and 1% penicillin/streptomycin. SMCs were grown in these media for 1-8 days; SMC number was assessed by a crystal violet-binding assay exactly parallel to that described above for ECs. Standard curves were linear from 0 to 20×10^3 SMCs/well (data not shown).

EC apoptosis experiments

Mouse ECs were plated at 7,500 per well onto 8-well culture slides (Nunc/Thermo), in medium A lacking FBS and supplemented with vehicle or recombinant mouse IL-9 (R&D Systems) at a final concentration of 600 pg/mL. ECs were incubated at 37 °C in a CO_2 incubator for 2 days and then processed for immunofluorescence microscopy.

ECs were fixed for 2 min in ethanol:formalin:water (75:15:10, vol/vol), rinsed thrice in phosphate-buffered saline (PBS, 3 min/wash), and then blocked for 30 min (25 °C) in "blocking buffer": 4% (vol/vol) FBS/0.2% (w/vol) gelatin/PBS. Next, ECs were incubated in blocking buffer containing rabbit monoclonal anti-cleaved caspase-3 diluted 1:25 (Cell Signaling, #9664) or non-immune rabbit IgG for 1 hr (25 °C), and then rinsed in PBS as above. ECs were then incubated for 1 hr (25 °C) in blocking buffer containing (a) FITC-conjugated sheep IgG targeting von Willebrand factor diluted 1:25 (Abcam, #ab8822) and (b) Alexa® 546-conjugated anti-rabbit IgG diluted 1:50 (Molecular Probes). After 3 rinses performed as above, slides were covered with Fluoromount-G (Southern Biotech) and coverslipped for microscopy. Non-immune rabbit IgG used as a primary IgG yielded no red immunofluorescence.

Human vein samples from arteriovenous fistulae (AVFs)

All procedures with human volunteers were approved by the Duke Institutional Review Board, under Protocol Number Pro00040569, and conformed to the principles outlined in the Declaration of Helsinki. All human subjects gave their informed consent prior to their inclusion in the study and collection of vein specimens. Vein specimens were obtained by a single surgeon (J. H. L.) from 5 humans with end-stage renal disease when they underwent two-stage basilic vein transposition AVF surgery or radiocephalic AVF surgery.[23] For two-stage basilic vein transposition, the basilic vein was anastomosed to the brachial artery and allowed to mature in place. Because the basilic vein resides deep within the arm (and therefore cannot be easily cannulated for hemodialysis), after maturation of the AVF, the AVF's basilic vein must be transposed to a subcutaneous location to facilitate access for hemodialysis. Thus, between 3 and 5 months after initial AVF creation, a second surgery detached the (arterialized) basilic vein from its original anastomosis, tunneled it under the skin, and reconnected it to the brachial artery at a new anastomosis.

Samples of "native vein," 3-5 mm in length, were obtained intraoperatively during the initial construction of the AVF. "AVF vein" samples were also obtained intraoperatively, when the arterialized basilic vein transposition. In one case, we procured an "AVF vein" sample 11 months following radiocephalic AVF construction, during surgery required for AVF revision. Native and AVF vein samples were embedded in OCT and frozen in the operating room, immediately after removal from each human volunteer. Serial frozen sections were stained with trichrome or, in pairs of "native" and "AVF" vein from single subjects, with primary IgGs targeting IL-9, IL-9Rα, mast cell tryptase, or no particular protein; sections were counterstained with Hoechst 33342 (DNA, blue). Immunofluorescence data were acquired and processed as described above for mouse vein samples.

Statistical analyses

All values were plotted in figures as means ± SE and cited in the text as means ± SD. GraphPad Prism® software was used to perform *t* tests (for comparing two groups), 1-way ANOVA with Tukey's post-hoc test for multiple comparisons (≥3 groups), or 2-way ANOVA with Sidak's post-hoc test for multiple comparisons. A p value of less than 0.05 was considered significant.

To analyze data from serum cytokine assays, the distributions of each cytokine were examined. We made 2 comparisons of "treatment" versus "control": (1) CKD mice versus control-GFR mice, and (2) anti-IL-9-IgG-injected CKD mice versus control IgG-injected CKD mice. We compared the medians between the treatment and control groups using the non-parametric Wilcoxon Test with

exact *p* value calculation, under the null hypothesis that there was no difference between the treatment and control groups. A conservative multiple comparisons correction for 23 independent cytokines was used to indicate a significant test: $p < 0.05/23$, or $p < 0.00217$.

SUPPLEMENTARY REFERENCES

1. Bro S, Moeller F, Andersen CB, Olgaard K, Nielsen LB. Increased expression of adhesion molecules in uremic atherosclerosis in apolipoprotein-E-deficient mice. *J Am Soc Nephrol* 2004;**15**:1495-1503.
2. Qi Z, Whitt I, Mehta A, Jin J, Zhao M, Harris RC, Fogo AB, Breyer MD. Serial determination of glomerular filtration rate in conscious mice using FITC-inulin clearance. *Am J Physiol Renal Physiol* 2004;**286**:F590-596.
3. Pedersen TX, Madsen M, Junker N, Christoffersen C, Vikesa J, Bro S, Hultgardh-Nilsson A, Nielsen LB. Osteopontin deficiency dampens the pro-atherogenic effect of uraemia. *Cardiovasc Res* 2013;**98**:352-359.
4. Bernardi S, Candido R, Toffoli B, Carretta R, Fabris B. Prevention of accelerated atherosclerosis by AT1 receptor blockade in experimental renal failure. *Nephrol Dial Transplant* 2011;**26**:832-838.
5. Ma LJ, Fogo AB. Model of robust induction of glomerulosclerosis in mice: importance of genetic background. *Kidney Int* 2003;**64**:350-355.
6. Gurley SB, Mach CL, Stegbauer J, Yang J, Snow KP, Hu A, Meyer TW, Coffman TM. Influence of genetic background on albuminuria and kidney injury in Ins2(+/C96Y) (Akita) mice. *Am J Physiol Renal Physiol* 2010;**298**:F788-795.
7. Zhang L, Hagen PO, Kisslo J, Peppel K, Freedman NJ. Neointimal hyperplasia rapidly reaches steady state in a novel murine vein graft model. *J Vasc Surg* 2002;**36**:824-832.
8. Zhang L, Freedman NJ, Brian L, Peppel K. Graft-extrinsic cells predominate in vein graft arterialization. *Arterioscler Thromb Vasc Biol* 2004;**24**:470-476.
9. Zhang L, Peppel K, Brian L, Chien L, Freedman NJ. Vein graft neointimal hyperplasia is exacerbated by tumor necrosis factor receptor-1 signaling in graft-intrinsic cells. *Arterioscler Thromb Vasc Biol* 2004;**24**:2277-2283.
10. Zhang L, Sivashanmugam P, Wu JH, Brian L, Exum ST, Freedman NJ, Peppel K. Tumor necrosis factor receptor-2 signaling attenuates vein graft neointima formation by promoting endothelial recovery. *Arterioscler Thromb Vasc Biol* 2008;**28**:284-289.
11. Zhang L, Brian L, Freedman NJ. Vein graft neointimal hyperplasia is exacerbated by CXCR4 signaling in vein graft-extrinsic cells. *J Vasc Surg* 2012;**56**:1390-1397.
12. Zhang L, Peppel K, Sivashanmugam P, Orman ES, Brian L, Exum ST, Freedman NJ. Expression of tumor necrosis factor receptor-1 in arterial wall cells promotes atherosclerosis. *Arterioscler Thromb Vasc Biol* 2007;**27**:1087-1094.
13. Bot I, de Jager SC, Zernecke A, Lindstedt KA, van Berkel TJ, Weber C, Biessen EA. Perivascular mast cells promote atherogenesis and induce plaque destabilization in apolipoprotein E-deficient mice. *Circulation* 2007;**115**:2516-2525.
14. Combs JW, Lagunoff D, Benditt EP. Differentiation and proliferation of embryonic mast cells of the rat. *J Cell Biol* 1965;**25**:577-592.

15. Shenoy SK, Lefkowitz RJ. Trafficking patterns of beta-arrestin and G protein-coupled receptors determined by the kinetics of β-arrestin deubiquitination. *J Biol Chem* 2003;**278**:14498-14506.

16. North AJ. Seeing is believing? A beginners' guide to practical pitfalls in image acquisition. *J Cell Biol* 2006;**172**:9-18.

17. Li H, Nourbakhsh B, Ciric B, Zhang GX, Rostami A. Neutralization of IL-9 ameliorates experimental autoimmune encephalomyelitis by decreasing the effector T cell population. *J Immunol* 2010;**185**:4095-4100.

18. Sheehan KC, Pinckard JK, Arthur CD, Dehner LP, Goeddel DV, Schreiber RD. Monoclonal antibodies specific for murine p55 and p75 tumor necrosis factor receptors: identification of a novel in vivo role for p75. *J Exp Med* 1995;**181**:607-617.

19. Yasuhara M, Fujita S, Arisue K, Kohda K, Hayashi C. A new enzymatic method to determine creatine. *Clin Chim Acta* 1982;**122**:181-188.

20. Burris D, Webster R, Sheriff S, Faroqui R, Levi M, Hawse JR, Amlal H. Estrogen directly and specifically downregulates NaPi-IIa through the activation of both estrogen receptor isoforms (ERα and ERβ) in rat kidney proximal tubule. *Am J Physiol Renal Physiol* 2015;**308**:F522-534.

21. Wang J, Sjoberg S, Tia V, Secco B, Chen H, Yang M, Sukhova GK, Shi GP. Pharmaceutical stabilization of mast cells attenuates experimental atherogenesis in low-density lipoprotein receptor-deficient mice. *Atherosclerosis* 2013;**229**:304-309.

22. Wu JH, Zhang L, Fanaroff AC, Cai X, Sharma KC, Brian L, Exum ST, Shenoy SK, Peppel K, Freedman NJ. G Protein-coupled receptor kinase-5 attenuates atherosclerosis by regulating receptor tyrosine kinases and 7-transmembrane receptors. *Arterioscler Thromb Vasc Biol* 2012;**32**:308-316.

23. Conte MS, Nugent HM, Gaccione P, Roy-Chaudhury P, Lawson JH. Influence of diabetes and perivascular allogeneic endothelial cell implants on arteriovenous fistula remodeling. *J Vasc Surg* 2011;**54**:1383-1389.

Table: Clinical Characteristics of Human Vein Donors

Subject	Native Vein	AVF Vein	AVF Maturation (months)	Age (y)	Ethnicity	Sex	Co-morbidities
1	Basilic	Mature	5	70	EA	M	HTN, DM2, CAD, CHF, HL
2	Basilic	Mature	3	48	AA	M	HTN, DM1, PAD
3	Cephalic	Mature and stenotic segments (from radiocephalic AVF revision)	11	32	AA	M	HTN, HIV
4	Basilic	Mature	4	47	EA	F	HTN, DM, PAD, CVA, CHF, HL
5	Basilic	Mature	4	31	LA	M	HTN, DM1

"AVF Maturation" denotes the time between the initial surgery (at which native vein was harvested) and the subsequent surgery (stage 2 of the brachiobasilic AVF or revision of the radiocephalic AVF).
Abbreviations: EA, European American; AA, African American; LA, Latino American; HTN, hypertension; DM2, type II diabetes mellitus; CAD, coronary artery disease; CHF, congestive heart failure; HL, hyperlipidemia; DM1, type I diabetes mellitus; PAD, peripheral artery disease; HIV, human immunodeficiency virus; CVA, cerebrovascular accident.

Table S1. Characteristics of human subjects from whom AVF veins were harvested during surgery. Vein specimens were obtained from 5 humans with end-stage renal disease undergoing 2-stage basilic vein transposition or radiocephalic AVF surgery: (a) at the initial construction of the AVF (*native* vein), and (b) 3-5 months following AVF construction, at the time of brachiobasilic AVF transposition, or 11 months following radiocephalic AVF construction, at the time of AVF revision—when vein arterialization had already taken place (*AVF* vein).

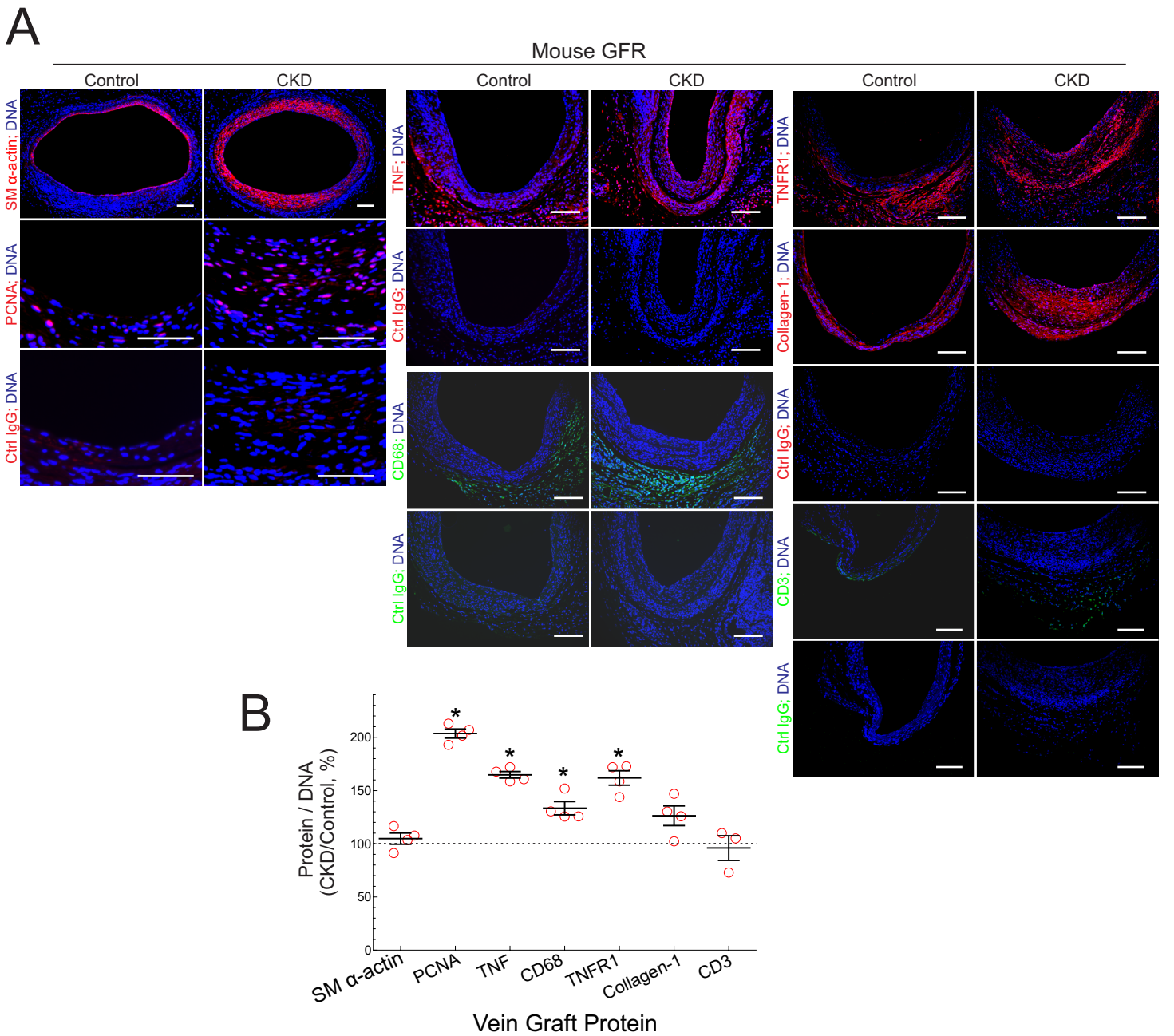

Figure S1. CKD augments vein graft neointimal hyperplasia and inflammation. (*A*) Serial sections of vein grafts from Figures 1 and 2 were immunostained for the indicated protein as in Figure 2, with protein-specific or isotype control IgGs from rabbit (PCNA), mouse (TNFR1, collagen I), rat (CD68), or goat (TNF, CD3). Vein grafts from control-GFR and CKD mice were stained batch-wise. Scale bars = 50 μm. (*B*) The ratios of red or green (protein) to blue (DNA) pixels in the vein graft wall were quantitated by Image J, and normalized to the cognate ratios obtained for control specimens in each staining cohort, to obtain "CKD/Control", plotted as means ± SE for 3-4 vein grafts in each GFR group. Compared with control: *, $p < 0.05$ (2-way ANOVA with Sidak post-hoc test).

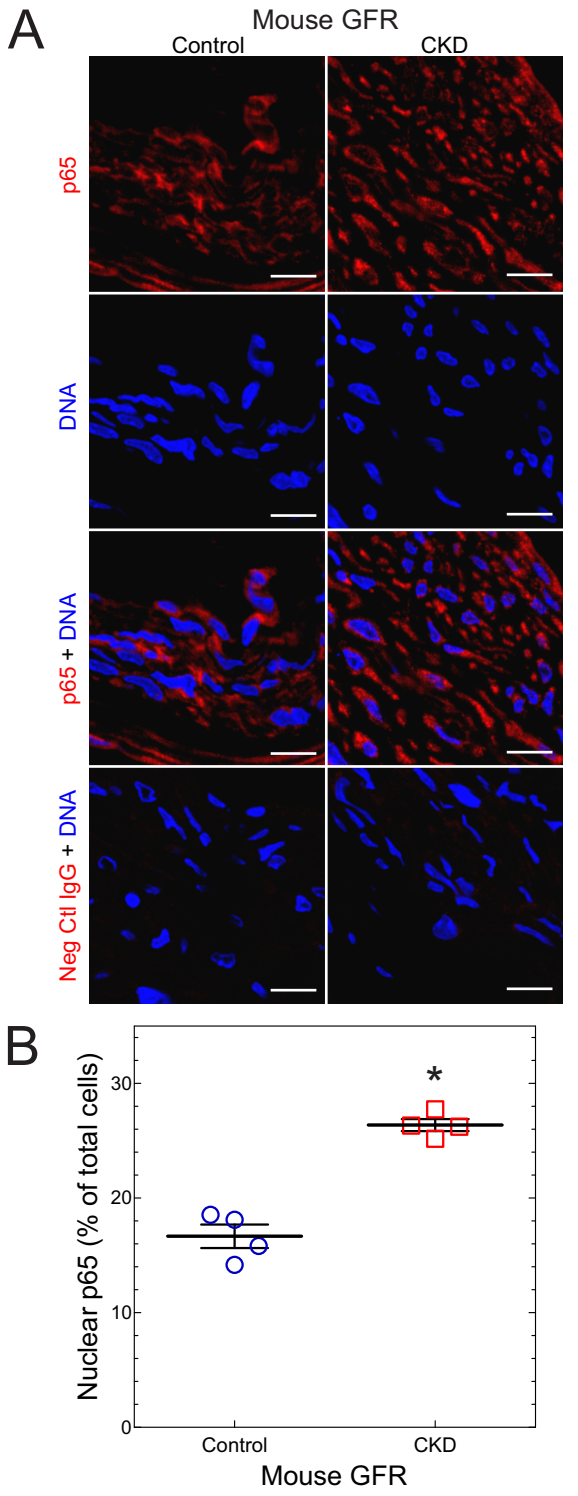

Figure S2. CKD augments NFκB activation in vein grafts. (*A*), Serial sections of vein grafts from Figure 2 and Supplementary Figure 1 were immunostained with rabbit IgG targeting the NFκB p65 subunit (*p65*) or no specific protein (*Neg Ctl IgG*). Alexa 546-conjugated anti-rabbit IgG and DRAQ5™ (for nuclear DNA) were used on all specimens. Specimens from control and CKD mice were stained concurrently, and imaged by confocal microscopy with identical settings (see Methods). (*B*), Neointimal and medial nuclei were counted manually by observers blinded to specimen identity (at least 200 per vein graft), and the percent of nuclei evincing red p65 staining was quantitated from 4 vein grafts of each GFR group, as indicated, with means ± SE. Compared with control: *, $p < 0.01$ (*t* test).

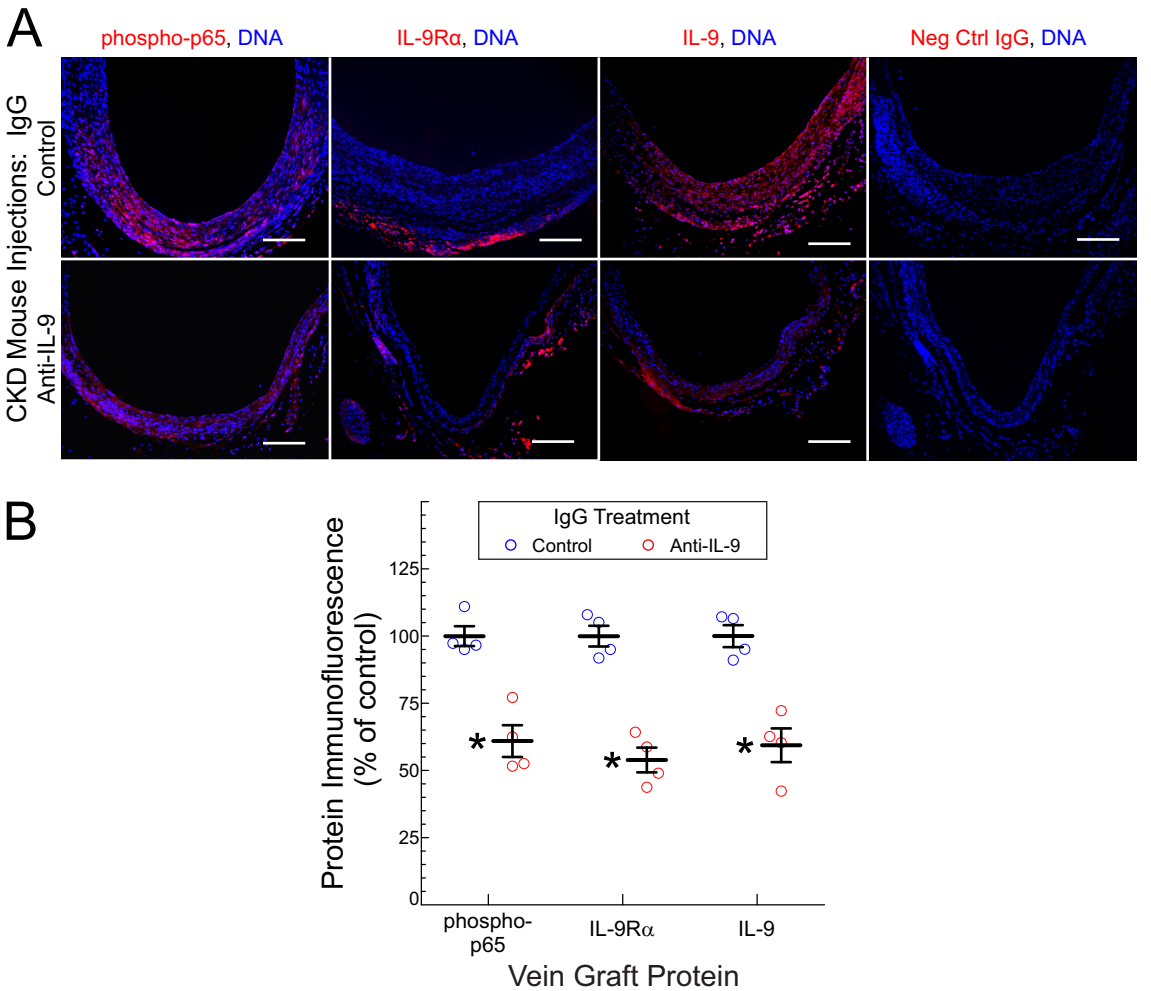

Figure S3. IL-9 exacerbates vein graft inflammation. (*A*) Serial sections of vein grafts from Figure 5 were stained with Hoechst 33342 (blue, DNA) and immunostained (red) with rabbit IgG specific for NFκB p65 phosphorylated on Ser536 (*phospho-p65*), IL-9 receptor-α (*IL-9Rα*), IL-9, or no particular protein (*Neg Control*). Scale bars = 50 μm. (*B*) Protein immunofluorescence throughout the vein graft wall was normalized to cognate DNA fluorescence intensity; resulting ratios were normalized within each staining group to the mean of samples from control IgG-injected CKD mice, to yield "% of control," plotted as means±S.E. of 4 vein grafts per group. Compared with control: *, $p < 0.05$ (2-way ANOVA with Sidak post-hoc test).

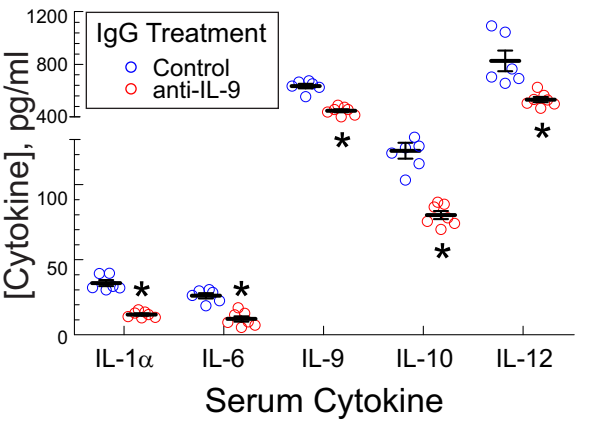

Figure S4. Inhibiting IL-9 reduces the serum levels of multiple cytokines. CKD mice were injected 3 times per week with anti-IL-9 IgG or isotype control IgG for 4 wk. Two to three days after the final IgG injections, mice were sacrificed for the harvest of vein grafts (Figure 5) and serum. Serum from each mouse was assayed for cytokines in triplicate by a single run of the Bio-Plex Pro™ Mouse Cytokine assay (as in Figure 3). Plotted are the means ± SE for the indicated serum cytokine levels in mice treated with control or anti-IL-9 IgG (n = 6-7/group). Compared with control IgG-injected mice: *, $p < 0.002$ (Wilcoxon Test).

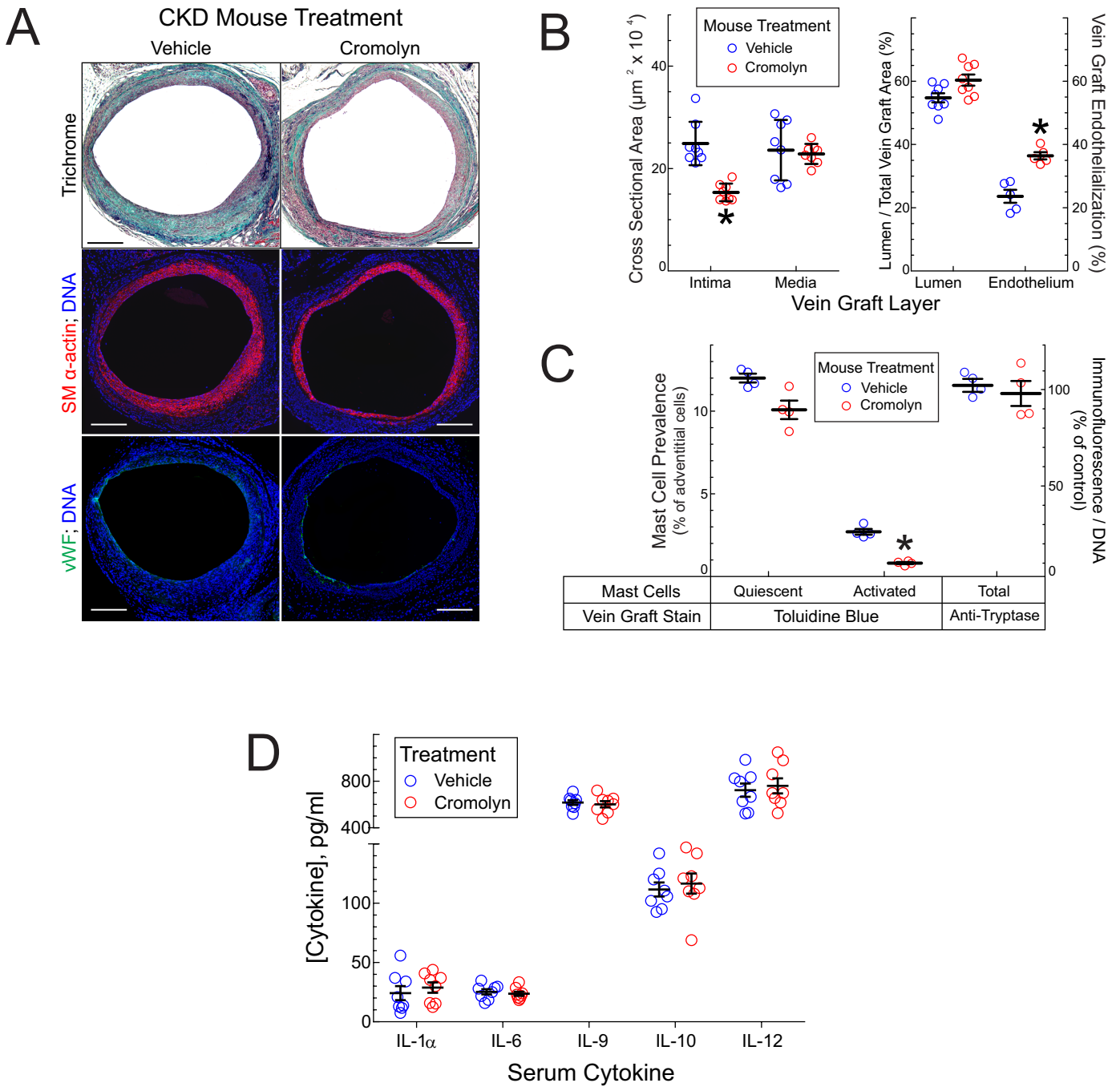

Figure S5. Inhibition of mast cell degranulation attenuates CKD-dependent vein graft disease. Mice were subjected to 5/6ths nephrectomy and vein graft surgery as in Figure 1. On the day prior to vein graft surgery and thrice weekly thereafter, mice were injected i.p. with PBS lacking (vehicle) or containing cromolyn sodium (50 mg/kg). Vein grafts were harvested 4 wk post-operatively, as in Figures 1 and 5. (*A*) Serial sections of perfusion-fixed vein grafts were stained with a modified Masson trichrome or immunofluorescently for smooth muscle (SM) α-actin or von Willebrand factor (vWF, green), along with Hoechst 33342 counterstain (blue, DNA). Scale bars = 100 μm. (*B*) The indicated cross sectional areas were calculated by planimetry and plotted as means ± SE from 8 mice in each group. For each vein graft, luminal area was normalized to cognate total vein graft cross-sectional area prior to plotting. "Vein graft endothelialization" was calculated as in Figure 1, and plotted as means ± SE from 5 mice in each group. Compared with control mice: *, $p < 0.05$. (*C*) Serial sections of vein grafts from panel A were stained with toluidine blue or anti-tryptase IgG to identify mast cells, as in Figure 4. The prevalence of quiescent and activated mast cells in vein grafts was assessed by toluidine blue staining as in Figure 4, and the prevalence of total mast cells was assessed by anti-tryptase staining and normalized to that found in vein grafts from vehicle-treated mice, as presented in Figure 4. Plotted are the means ± S.E. of 4 vein grafts per group (at least 100 adventitial mast cells were counted per specimen). Compared with vein grafts from vehicle-treated mice: *, $p < 0.05$ (2-way ANOVA with Sidak post-hoc test). (*D*) Serum from each mouse depicted in panel A was assayed for cytokines in triplicate by a single run of the Bio-Plex Pro™ Mouse Cytokine assay (as in Figure 3 and Supplementary Figure 4). Average values for each mouse are plotted, along with means ± SE for the indicated serum cytokine levels in mice treated with vehicle or cromolyn (n = 8/group).